Pergamon

Materials Research Bulletin 35 (2000) 2135–2143

Materials
Research
Bulletin

Synthesis of ferroelectric nanocrystalline $SrBi_2Ta_2O_9$ powder by the colloid-gel process

Chung-Hsin Lu*, Susanta Kumar Saha

Department of Chemical Engineering, National Taiwan University, Taipei, Taiwan, R.O.C.

(Refereed)
Received 25 October 1999; accepted 23 March 2000

Abstract

An innovative colloid-gel process using inorganic salts as starting materials has been successfully developed for preparing ferroelectric strontium bismuth tantalate ($SrBi_2Ta_2O_9$) powder. This new technique began with the preparation of a mixture of $Ta(OH)_5$ colloid with the aqueous solutions of strontium and bismuth cations, followed by the addition of ethylene glycol and citric acid as gel-forming reagents. During the calcination process the fluorite phase was formed as an intermediate that was subsequently converted into the $SrBi_2Ta_2O_9$ phase. After calcination at 750°C, pure ultrafine $SrBi_2Ta_2O_9$ polycrystalline powder with a narrow particle size distribution was obtained. The primary particle size of the obtained $SrBi_2Ta_2O_9$ powder was around 40 nm. In comparison with the solid-state reaction, the newly developed colloid-gel process significantly reduces the heating temperature for synthesizing $SrBi_2Ta_2O_9$, as well as the particle size of the obtained powder. © 2001 Elsevier Science Ltd. All rights reserved.

Keywords: A. Ceramics; A. Electronic materials; B. Sol-gel chemistry; C. Electron microscopy; C. X-ray diffraction

---

1. Introduction

In recent years, bismuth layered-structured ferroelectric materials such as $SrBi_2Ta_2O_9$ and $Bi_4Ti_3O_{12}$ have become important candidates for application in nonvolatile ferroelectric random access memories (FeRAM) due to their low coercive field and low leakage current density. $SrBi_2Ta_2O_9$ has great potential for use in FeRAM devices because it exhibits fatigue-free characteristics up to about 10^{12} switching cycles [1–3]. $SrBi_2Ta_2O_9$ belongs to the family of so-called multilayered interstitial compounds having the general formula

---

* Corresponding author. Fax: +886-2-2362-3040.

PII: S0025-5408(00)00422-0

$(Bi_2O_2)^{2+}(A_{n-1}B_nO_{3n+1})^{2-}$. The structure of $SrBi_2Ta_2O_9$ contains a stacking along the c-axis of two perovskite-like TaO_6 octahedron units between $(Bi_2O_2)^{2+}$ layers, whereas strontium cations are located in the space between TaO_6 octahedrons. Aurivillius first synthesized the ceramic form of $SrBi_2Ta_2O_9$ [4], and Smolenskii [5] and Subbarao [6] later studied its dielectric properties and phase transformation. Extensive studies have been carried out examining the formation of $SrBi_2Ta_2O_9$ films by different processes [7–15]; however, the literature regarding the preparation of $SrBi_2Ta_2O_9$ powder is very limited [6,16,17]. The main problem in using the conventional solid-state method for synthesizing $SrBi_2Ta_2O_9$ ceramic powder is the formation of large grains that affect the sintering properties of $SrBi_2Ta_2O_9$. Few studies have focused on synthesizing the single-phase $SrBi_2Ta_2O_9$ powder with fine particle size. Lu and Lee [16] reported a solid-state two-step synthesis method using $SrCO_3$ and $BiTaO_4$. However, the solid-state method requires calcination at high temperature, which causes coarsening of the powder.

Various chemical methods have been developed for the synthesis of pure, single-phase mixed-oxide powders with controlled powder characteristics. One of the more successful techniques for high-quality ceramic powder synthesis is the so-called Pechini process [18], which is a solution-polymerization route. In general, the process relies on the ability of certain organic acids (e.g., citric acid) to chelate metal ions [19–21]. Then, with the help of a polyhydroxy alcohol (e.g., ethylene glycol), the chelates undergo polyesterification when heated [22]. The polyesterification reaction results in a polymerized resin that has the various cations distributed uniformly in stoichiometric proportions. The polymerized resin that contains the chelated cations is the preceramic powder, which can then be calcined to obtain the target ceramic powder. Since its invention in the 1960s, the Pechini method (and slight variations thereof) has been used to produce niobates, titanates, zirconates, chromites, ferrites, manganates, aluminates, cobaltites, and silicates [19–24].

The purpose of this study was to develop a new chemical process for preparing ultrafine $SrBi_2Ta_2O_9$ powder using inorganic salts as starting materials rather than alkoxides. The developed process can avoid the complex handling and refluxing of alkoxides. As a suitable water soluble salt of tantalum is not available, a colloidal suspension of $Ta(OH)_5$ was used as the source of tantalum species. Citric acid and ethylene glycol were used to maintain the homogeneity of the precursor powder. The formation processes of $SrBi_2Ta_2O_9$ in this process were investigated for adjusting the calcination conditions to produce the pure phase. The microstructural development of the powder during heating was also examined.

2. Experimental

The flow chart for preparing $SrBi_2Ta_2O_9$ powder is illustrated in Fig. 1. The inorganic salts, tantalum(V) chloride (99.8%, Aldrich Chemical Company, Milwaukee, WI), bismuth(III) nitrate pentahydrate (99.5%, Nacalai Tesque, Kyoto, Japan), and strontium nitrate (99.8%, Aldrich Chemical Company), were used as raw materials to prepare $SrBi_2Ta_2O_9$. To remove chloride ions from the starting material, a colloidal suspension of tantalum(V) chloride was prepared in water, followed by the addition of ammonia to precipitate tantalum hydroxide. The tantalum hydroxide precipitate was filtered and repeatedly washed with

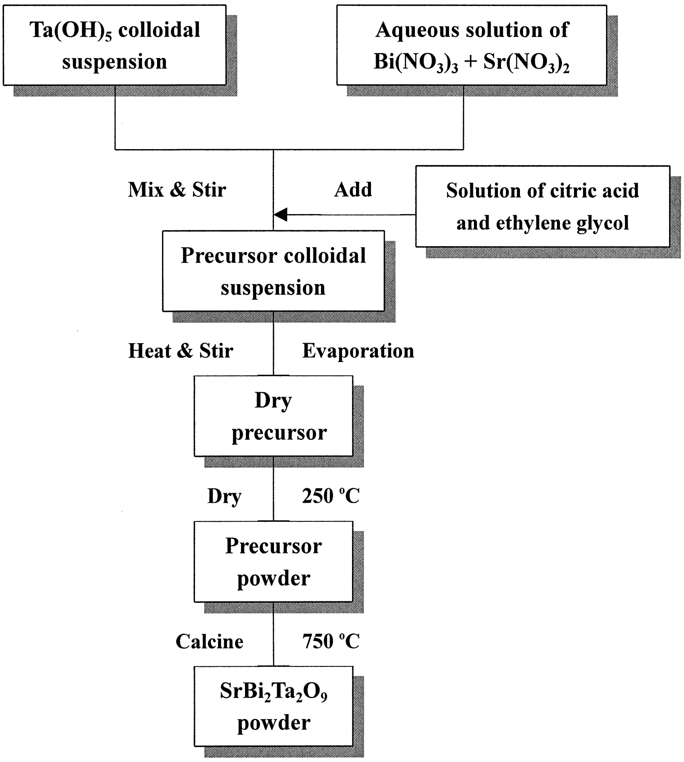

Fig. 1. Flow chart for the preparation of $SrBi_2Ta_2O_9$ powder.

deionized water. Clear solutions of bismuth and strontium nitrate were prepared separately. These solutions were added into the colloidal suspension of tantalum hydroxide according to the molar ratio Sr^{2+}:Bi^{3+}:Ta^{5+} = 1:2:2. The colloidal suspension of tantalum hydroxide was used as the source of tantalum due to the unavailability of suitable water-soluble common salt. Citric acid and ethylene glycol with a ratio of 1:1 were added into the mixed sol solution. The total metal ion to citric acid molar ratio was maintained at 1:2. The sol solution was evaporated at 250°C to obtain the precursor powder. This precursor powder was quenched and calcined in air in a muffle furnace at elevated temperatures.

To verify the reaction occurring in the precursor powder, thermogravimetric and differential thermal analyses (TG/DTA) was conducted using an Ulvac DTG 7000. Infrared spectra of calcined powder were examined in a KBr medium using a Bio-Rad FTIR spectrophotometer. The phase identification and structural analysis for the heat-treated samples were performed by powder X-ray diffraction using a Mac X-ray diffractometer. The crystallite size of the calcined powder was calculated from the broadening at half maximum of the X-ray spectral (115) peak of $SrBi_2Ta_2O_9$ based on Scherrer's formula [25]. The relative amounts of fluorite phase and $SrBi_2Ta_2O_9$ present in the heated samples were estimated based on the (111) diffraction peak of fluorite phase and the (115) diffraction peak of $SrBi_2Ta_2O_9$. The particle size and morphology of the calcined powders were examined by scanning electron microscopy (SEM) using a Hitachi S-800 microscope.

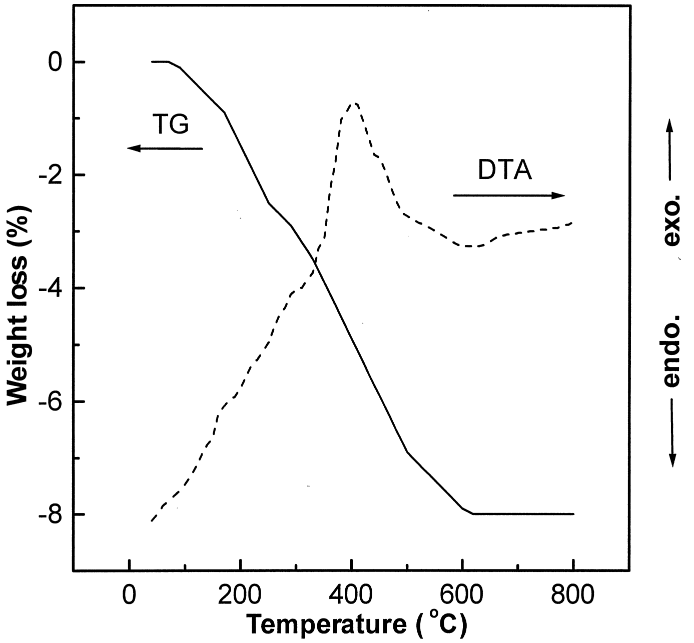

Fig. 2. TG/DTA trace at a heating rate of 10°C/min in air for the precursor powder of $SrBi_2Ta_2O_9$.

3. Results and discussion

TG/DTA results for the precursor powder are shown in Fig. 2. A large exothermic reaction was observed in DTA at about 400°C, which was caused by the combustion of the organic species present in the precursors. This indicates the incomplete removal of the residual organic species and nitrates by redox reaction in the previous drying process at 250°C to obtain the precursor powder. The TG spectrum showed a steady loss of mass up to 600°C; after that, no significant change of mass was found.

Spectroscopic analysis using FTIR was conducted on the precursor and quenched powders. Fig. 3 shows the FTIR results. For the precursor powder, two strong bands appeared at 854 and 1463 cm^{-1}, indicating the presence of carbonate groups. Upon quenching at 600°C, the band intensity of the carbonate group was reduced significantly, but the bands remained visible. All carbonate groups disappeared after the sample was heated at 700°C, at which the precursor attained a stable weight, as shown on the TGA curve (Fig. 2). At ≥700°C, two large bands appeared at 560 and 630 cm^{-1}, revealing the formation of a large amount of $SrBi_2Ta_2O_9$.

The precursor powder was calcined at elevated temperatures for various duration times to examine the formation of $SrBi_2Ta_2O_9$. The XRD patterns for the samples calcined for 2 h are shown in Fig. 4. Fluorite phase and an unknown compound were formed as intermediate phases after calcination at 500°C. At this temperature, the formation of $SrBi_2Ta_2O_9$ has also started. The relative amounts of fluorite phase and $SrBi_2Ta_2O_9$ are shown in Fig. 5. With an increase in the heating temperature, the amount of $SrBi_2Ta_2O_9$ rapidly increased, accompanied with a corresponding decrease in the amount of fluorite phase. After calcination at 750°C for 2 h, the single phase $SrBi_2Ta_2O_9$ with a well-developed layered structure was obtained. The formation of

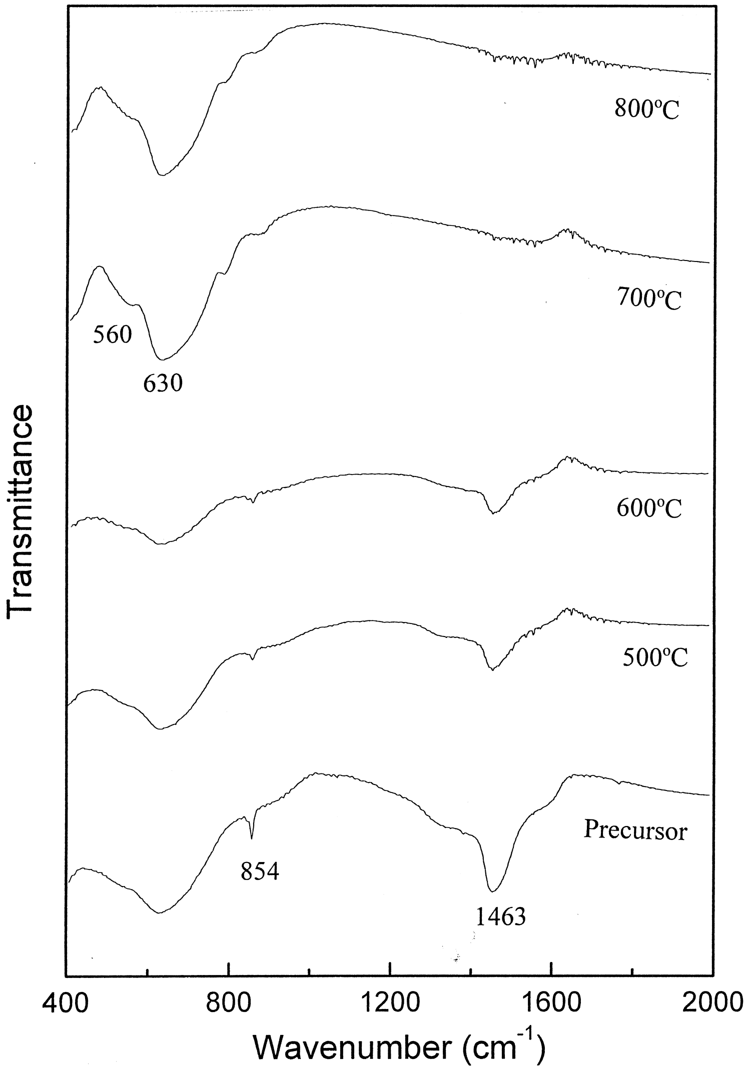

Fig. 3. FTIR spectra of precursor and quenched powder of $SrBi_2Ta_2O_9$.

fluorite phase was also found while heating the sol-gel-derived $SrBi_2Ta_2O_9$ films [26,27]. The $SrBi_2Ta_2O_9$ phase remained stable after calcining the sample at 900°C for 6 h. In the previously reported colloid-emulsion technique [28], pyrochlore phase was formed as an intermediate that was ultimately converted into single phase $SrBi_2Ta_2O_9$. In the present method, the fluorite phase serves as the intermediate. Extensive studies are needed to reveal the possible reasons for the formation of different types of intermediates.

Fig. 6 shows the average crystallite size, calculated using Scherrer's equation, as a function of calcination temperature from 700 to 900°C. The average crystallite size of the powder calcined at 700°C for 2 h was 19 nm, which increased to 23 nm when the calcination temperature was raised to 800°C. Crystallite size, as well as the order of crystallinity,

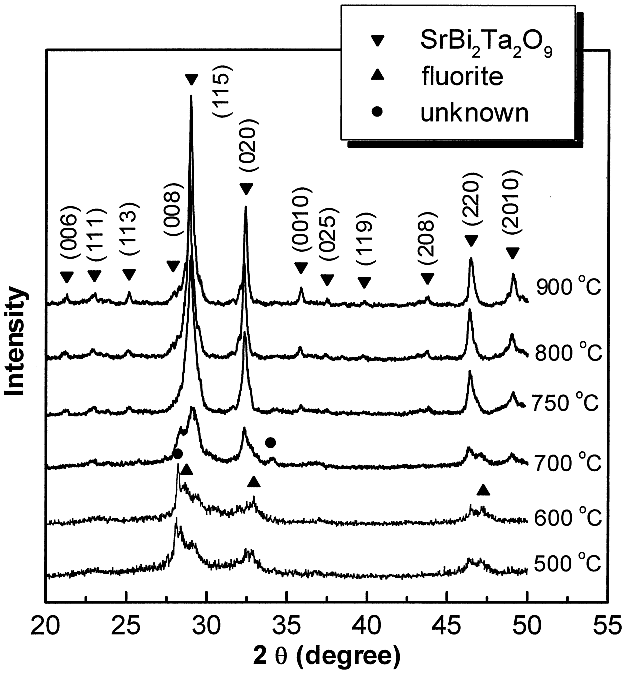

Fig. 4. XRD patterns for the samples of $SrBi_2Ta_2O_9$ calcined for 2 h at various temperatures.

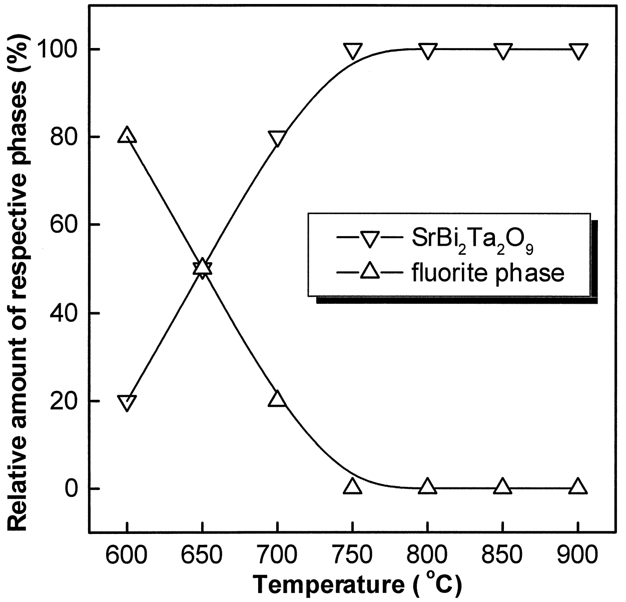

Fig. 5. Relative amount of resultant phases in the samples of $SrBi_2Ta_2O_9$ calcined at different temperatures for 2 h.

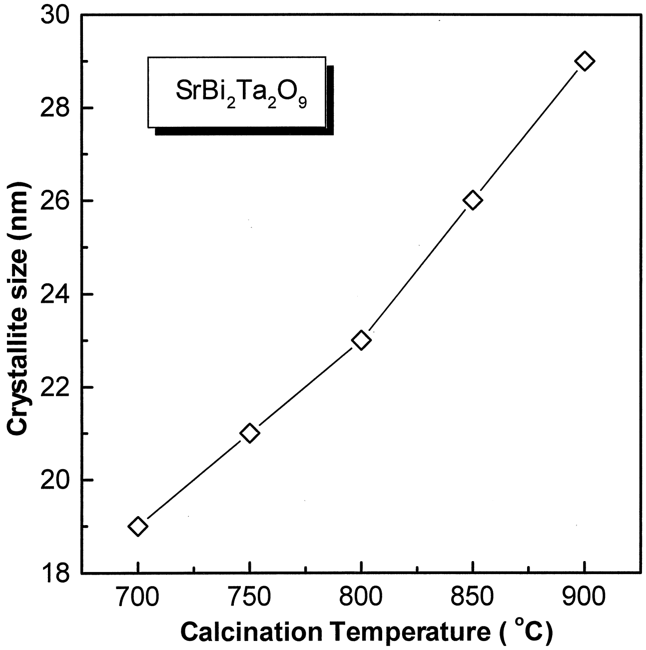

Fig. 6. Crystallite size of $SrBi_2Ta_2O_9$ as a function of calcination temperature.

increased with increase in temperature. The crystallite size was found to be 29 nm for powder calcined at 900°C.

The particle size and morphology of precursor and calcined powders were examined by scanning electron microscopy. As shown in Fig. 7a, the primary particle size of the precursor powder was very small, with an average size of 30 nm. The formation of nanosized particles might be due to the decomposition of the organic species present in the gel, along with the evolution of gases. Particle morphology of calcined powders (750°C for 2 h) was roughly spherical, with an average primary particle size around 40 nm (see Fig. 7b). Particle size increased with an increase in calcination temperature, and the average primary particle size for 850°C-calcined powder was about 70 nm. The primary particle sizes of the calcined powders were comparable to those obtained by the colloid-emulsion technique [28], but relatively small with respect to those obtained by the solid-state method.

In the previously reported two-step solid-state method [16], the single phase $SrBi_2Ta_2O_9$ was formed by calcining the mixed powder at 800°C. One of the precursors in that method was $BiTaO_4$, which was prepared by milling the respective oxides for 48 h followed by calcination at 900°C. In the colloid-gel method, the step of preparing $BiTaO_4$ precursor and the time-consuming milling process has been avoided. The temperature for the formation of pure single phase $SrBi_2Ta_2O_9$ was also reduced to 750°C in this method. In addition, the morphology of powder obtained through the solid-state method was rather hard agglomerates with large particles in comparison with the soft agglomerate powder of nanosized particles with narrow size distribution obtained by the present colloid-gel technique.

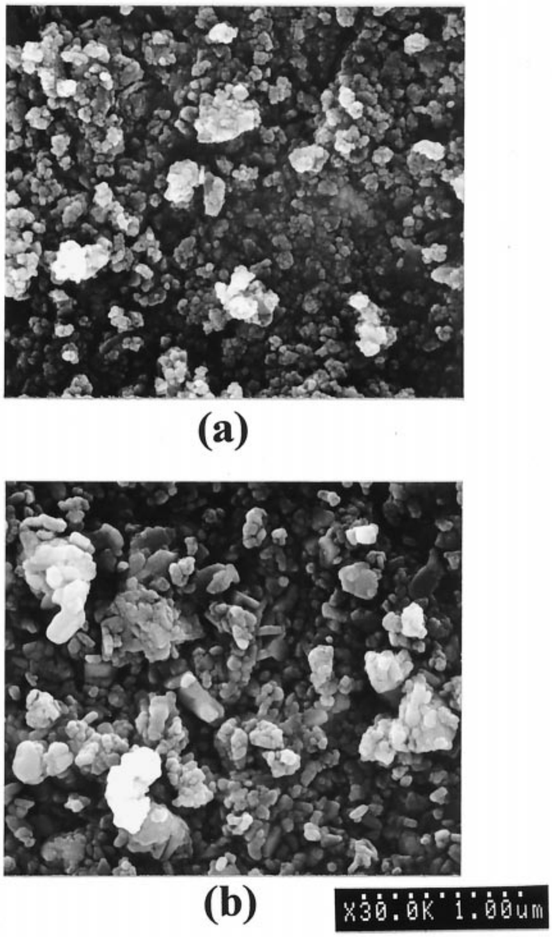

Fig. 7. Scanning electron micrograph of (a) precursor powder, and (b) $SrBi_2Ta_2O_9$ powder calcined at 750°C for 2 h.

4. Conclusions

Pure $SrBi_2Ta_2O_9$ powder was synthesized via a newly developed colloid-gel method. This technique is technically simple, compared with the conventional sol-gel method using alkoxides as raw materials. The materials used in the colloid-gel process are commonly available inorganic salts that do not require an inert environment for handling. During the calcination process of the precursor powder, fluorite phase coexisted with layered perovskite $SrBi_2Ta_2O_9$ phase. Formation of pure single phase $SrBi_2Ta_2O_9$ powder was completed by calcining the precursor powder at as low as 750°C for 2 h. With an increase in the calcination temperature, the order of crystallinity, crystallite size, as well as particle size increased. The average primary particle size of $SrBi_2Ta_2O_9$ synthesized at 750°C was 40 nm. As a result, monophasic nano-sized $SrBi_2Ta_2O_9$ powder was successfully prepared in this study.

Acknowledgments

The authors would like to acknowledge Mr. Chih-Yuan Tang and Miss Ching-Yen Lin in the Advanced Instrument Center in National Taiwan University for helping to analyze the microstructure of prepared powder. The authors would also like to thank the Chinese Petroleum Co. and the National Science Council, Taiwan, the Republic of China, for financial support of this research under contract No. NSC 88-CPC-E002-005.

References

[1] J.F. Scott, C.A. De Araujo Paz, Science 246 (1989) 1400–1405.
[2] C.A. De Araujo Paz, J.D. Cuchiaro, M.C. Scott, L.D. Mcmillan, Inter. Patent Appl. WO93/12542, 1993.
[3] J.F. Scott, F.M. Ross, C.A. De Araujo Paz, M.C. Scott, M. Huffman, Mater Res Soc Bull 21 (1996) 33–39.
[4] B. Aurivillus, Ark Kemi 54 (1949) 463–480.
[5] G.A. Smolenskii, V.A. Isupov, A.I. Agranovskaya, Fiz Tverdogo Tela 3 (1961) 895–901.
[6] E.C. Subbarao, J Phys Chem Solids 23 (1962) 665–676.
[7] S.S. Park, C.H. Yang, S.G. Yoon, J.H. Ahn, H.G. Kim, J Electrochem Soc 144 (1997) 2855–2858.
[8] H.M. Yang, J.S. Luo, W.T. Lin, J Mater Res 12 (1997) 1145–1151.
[9] S.B. Desu, D.P. Vijay, X. Zhang, B.P. He, Appl Phys Lett 69 (1996) 1719–1721.
[10] K. Amanuma, T. Hase, Y. Miyasaka, Appl Phys Lett 66 (1995) 221–223.
[11] P.Y. Chu, R.E. Jones Jr., P. Zurcher, D.J. Taylor, B. Jiang, S.L. Gillespie, Y.T. Lii, J Mater Res 11 (1996) 1065–1069.
[12] C.H. Lu, B.K. Fang, J Mater Res 12 (1997) 2104–2110.
[13] T. Li, Y. Zhu, S.B. Desu, C.H. Peng, M. Nagata, Appl Phys Lett 68 (1996) 616–619.
[14] T.J. Boyle, C.D. Buchheit, M.A. Rodriguez, H.N. Al-Shareef, B.A. Hernandez, B. Scott, J.W. Ziller, J Mater Res 11 (1996) 2274–2281.
[15] K. Kato, C. Zheng, J.M. Finder, S.K. Dey, K. Torii, J Am Ceram Soc 81 (1998) 1869–1875.
[16] C.H. Lu, J.T. Lee, Ceram Int 24 (1998) 285–291.
[17] C.H. Lu, Y.C. Chen, J Euro Ceram Soc 19 (1999) 2909–2915.
[18] M.P. Pechini, U.S. Patent No. 3,330,697, 1967.
[19] P.A. Lessing, Am Ceram Soc Bull 68 (1989) 1002–1007.
[20] H.U. Anderson, M.J. Pennell, J.P. Guha, in: G.L. Messing, K.L. Mazdiyasni, J.W. McCauley, R.A. Haber (Eds.), Advances in Ceramics, Vol. 21, American Ceramic Society, Westerville, OH, 1986, pp. 91–99.
[21] N.G. Eror, H.U. Anderson, in: C.J. Brinker, D.E. Clark, D.R. Ulrich (Eds.), Better Ceramics through Chemistry II, Materials Research Society, Pittsburgh, PA, 1986, pp. 571–577.
[22] M.A. Gulgun, W.M. Kriven, in: J.J. Kingsley, C.H. Schilling, J.H. Adair (Eds.), Ceramic Transactions, Vol. 62, American Ceramic Society, Westerville, OH, 1995, pp. 57–66.
[23] M.A. Gulgun, O.O. Popoola, W.M. Kriven, J Am Ceram Soc 77 (1994) 531–539.
[24] W. Liu, G.C. Farrington, F. Chaput, B. Dunn, J Electrochem Soc 143 (1996) 879–884.
[25] H.P. Klug, L.E. Alexander, X-ray Diffraction Procedures for Polycrystalline and Amorphous Materials, Wiley, New York, 1954, p. 491.
[26] T. Osaka, A. Sakakibara, T. Seki, S. Ono, I. Koiwa, A. Hashimoto, Jpn J Appl Phys 37 (1998) 597–601.
[27] M.A. Rodriguez, T.J. Boyle, B.A. Hernandez, C.D. Buchheit, M.O. Eatough, J Mater Res 11 (1996) 2282–2287.
[28] C. H. Lu, S. K. Saha, Mater Lett 42 (2000) 150–154.